

**Ground States of Crystalline Caps: Generalized Jellium on Curved Space**


Siyu Li and Roya Zandi

*Department of Physics and Astronomy, University of California, Riverside, California 92521, USA*

Alex Travesset

*Department of Physics and Astronomy, Iowa State University and Ames Lab, Ames, Iowa 50011, USA*

Gregory M. Grason

*Department of Polymer Science and Engineering, University of Massachusetts, Amherst, Massachusetts 01003, USA* (Received 7 June 2019; published 30 September 2019)

We study the ground states of crystals on spherical surfaces. These ground states consist of positive disclination defects in structures spanning from flat and weakly curved caps to closed shells. Comparing two continuum theories and one discrete-lattice simulation, we first investigate the transition between defect-free caps to single-disclination ground states and show it to be continuous and symmetry breaking. Further, we show that ground states adopt icosahedral subgroup symmetries across the full range of curvatures, even far from the closure of complete shells. While superficially similar to other models of 2D “jellium” (e.g., superconducting disks and 2D Wigner crystals), the interplay between the free edge of caps and the non-Euclidean geometry of its embedding leads to nontrivial ground state behavior that is without counterpart in planar jellium models.

DOI: [10.1103/PhysRevLett.123.145501](https://doi.org/10.1103/PhysRevLett.123.145501)

Spherical crystals are elementary models of geometric frustration in materials, with broad realizations from fullerenes and protein cages to coated droplets and solid-domains in multicomponent lipid vesicles [1–9]. The long-standing problem of finding the ground state of  $N$  particles covering the sphere, known as the generalized Thomson problem [10,11], derives its complexity from the conflict between equitriangular order and nonzero (positive) Gaussian curvature [12–15]. For closed shells, topology dictates the total charge of disclinations (i.e., sites deviating from sixfold coordination) to be  $\sum_{i=1}^{n_d} q_\alpha = 12$ , which for the simplest case of only fivefold defects ( $q_\alpha = +1$ ) constrains the number of disclinations to  $n_d = 12$  [14,16,17]. Considerable progress has been made by optimizing, classifying, and rationalizing the patterns of defects of closed shells [11,18–20]. In contrast, the defect ground states of partially closed crystalline shells, or *crystalline caps*, that span the gap between defect-free planar crystals and closed shells, remain unresolved [21–24].

Unlike closed shells, the number of defects in the interior of crystalline caps is not topologically constrained. Disclinations can be created and destroyed at the free boundary of the cap, adjusting the number in accordance with energetic considerations deriving from elastic screening by curvature-induced stresses [6,25–28]. In this vein, ground states of crystalline caps may be described by a *generalized jellium* (GJ) model, in which disclinations act as point sources of elastic stress in a background of continuous “neutralizing charge” deriving from Gaussian

curvature [12]. While the most familiar examples of GJ describe bulk phases like the Wigner crystal [29,30] or Abrikosov lattice of type-II superconductors [31–33], many scenarios are described by finite domains of homogeneously charged backgrounds punctuated by a finite number of neutralizing point or line charges. For example, under an increasing magnetic field, the ground state wave function of 2D superconducting disks exhibit a complex sequence of transitions in the number and symmetry of vortices [32,33], deriving from the incommensurability of the net applied flux with the quantized flux per vortex.

Although superficially similar to planar GJ models, crystalline caps are distinguished by their non-Euclidean (elliptic) geometry that alters the relationship between shape and length of the free boundary to the cap area. The effect of free boundaries can be thought in terms of “virtual” disclination charge, induced by vanishing elastic stress at the free cap edge. Because virtual charges also partially screen defect-induced stress, the optimal number of defects does not simply derive from the often invoked “neutrality condition” between Gaussian curvature and disclination charge [6]. In this Letter, we describe the spectrum of defect ground states of crystalline caps using a combination of continuum elasticity theory and simulation models. We show that geometrically nonlinear effects at the free edges give rise to a novel continuous transition from the defect-free interiors to a trapped central disclination as well as the soft, near-edge trapping of low-energy defects. This latter mechanism leads to a nontrivial sequence of

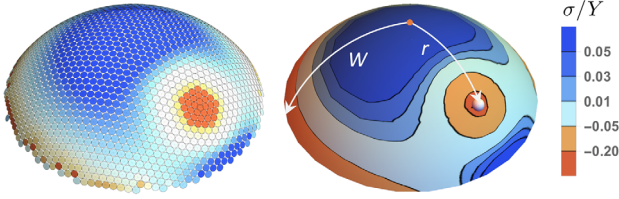


FIG. 1. Stress map in a crystalline cap with an off-center fivefold disclination located at  $r = 0.6W$  from Eq. (4) (left) and covariant theory, Eq. (2) (right).

defect ground states, which is characterized by a nonmonotonic dependence of a number of interior defects on the integrated Gaussian curvature, or sphere coverage, of the cap. Finally, we show that the non-Euclidean embedding of the GJ problem on the cap is essential for the emergence of a defect in ground states with symmetries commensurate with the icosahedral symmetry of closed shells (e.g., the Thomson problem [19]).

We consider a hexagonal crystal on a sphere of radius  $R$  extending a radial distance  $W = \theta_c R$  from its center to its free edge, see Figs. 1 and S7 [34]. While brittle crystallization on spheres may give rise to elastic instabilities of the boundary shape [25,35–37], here we consider the limit of large edge energy [38], where the crystal boundary remains axisymmetric. Such conditions are realized both in growth pathways of nanocrystalline shells [4,16,24,39] as well as crystalline “patch” domains in fluid-solid phase separated vesicles [8,9]. Furthermore, we restrict our attention to ground states that possess only  $q_\alpha = +1$  (fivefold) disclinations in an otherwise hexagonal bulk order, neglecting the possibilities of dislocations chains or “scars” that become energetically favorable when the lattice spacing  $a$  becomes sufficiently small compared to  $W$  [6,14,21].

The elastic energy takes the form

$$F = \frac{1}{2Y} \int d^2\mathbf{x} \sqrt{g} (\Delta\chi)^2, \quad (1)$$

where  $\sqrt{g}$  is the metric induced in the spherical cap and  $\chi$  is the Airy stress function, which encodes the elastic intracrystal stress [see the Supplemental Material, Eqs. (S9)–(S11)], and satisfies [14]

$$\frac{1}{Y} \Delta^2 \chi(\mathbf{x}) = s(\mathbf{x}) - K(\mathbf{x}), \quad (2)$$

where  $K(\mathbf{x})$  is the Gaussian curvature,  $\Delta = (1/\sqrt{g})\partial_i(\sqrt{g}g^{ij}\partial_j)$  is the Laplacian on a 2D surface with metric  $g_{ij}$ , and

$$s(\mathbf{x}) = \frac{\pi}{3\sqrt{g}} \sum_{\alpha=1}^{n_d} q_\alpha \delta(\mathbf{x} - \mathbf{x}_\alpha) \quad (3)$$

is the disclination density, composed of  $n_d$  disclinations possessing  $q_\alpha = +1$ , the topological charge per single

fivefold defect (i.e., with wedge angle  $\pi q_\alpha/3$  per defect). The effect of the free boundary motion is captured by imposing vanishing normal stress at the cap edge on solutions for  $\chi$ . Strictly speaking, caps are topologically equivalent to the disk (until the point of closure) which requires a fixed balance between disclinations in the bulk and on the boundary (i.e., the creation of an interior site with only five bonds requires decreasing the net number of three-bond edge sites) [17]. Notwithstanding this necessity of such “edge disclinations,” stress screening by the free boundary implies that the elastic effect of defects *vanishes* as they approach the boundary. Hence, energetics are sensitive only to *interior defects*.

The elastic energy of multidisclination configurations in caps were previously computed [40] for the so-called Föppl–van Kármán (FvK) limit [27,28], strictly justified in the limit of small slopes [41]. The FvK limit corresponds to approximating the metric  $g_{ij}$  to be planar in the Laplacian while retaining  $K(\mathbf{x}) = 1/R^2$  as a homogeneous source for Airy stress on the right hand side of Eq. (2). While the FvK theory is tractable for axisymmetric caps with arbitrary defect arrangements [23,42], the small-slope limit (i.e.,  $\theta_c \ll 1$ ) is not satisfied for nearly all of curvatures where defects are energetically favored. Indeed, as we show below, this approximation leads to both quantitative and qualitative errors in the ground state, making accurate predictions for the full range of curvature, from flat to closed shells, inaccessible to the FvK theory. Recently, the fully covariant elasticity theory of caps has been developed [24,43], building from elements in the theory of incompatible elasticity [44,45], and, more crucially, allowing for the computation of the energy of arbitrarily complex, multidefect configurations (see the Supplemental Material [34]). This approach, which hereon we will refer to as LF (Lagrange formalism) [43], captures the full geometric nonlinearity of the cap shape through incorporation of the spherical metric in the deformed state [i.e.,  $g_{rr} = 1$ ,  $g_{r\phi} = 0$ ,  $g_{\phi\phi} = R^2 \sin^2(r/R)$ ] while evaluating the Laplacian and area integral in Eq. (1). We note that the LF theory neglects higher-order contributions to in plane strains deriving from disclinations (beyond  $s^2$ ) [43]. While this approximation slightly modifies the near-field defect stresses, the LF theory captures the full nonlinearity of the spherical embedding and is otherwise tractable for comparing a spectrum of putative defect ground states of variable number, symmetry, and position.

In the context of the GJ models, the FvK model is the biharmonic analog of the 2D “electrostatic” theory of superconducting disks, that is, generalized by the longer-range interactions between monopoles in the biharmonic theory (i.e., interactions grow with separation  $r$  as  $\sim r^2 \ln r$ , in comparison to  $\ln r$  for 2D Coulomb [46]). In comparison, the LF theory embeds the “biharmonic electrostatics” problem in a non-Euclidean geometry, via the incorporation of spherical Laplacian and metrics in Eqs. (1)–(3). The effect of

the reduced geodesic separation between disclinations embedded on spheres, in combination with reduction of the perimeter to domain size ratio for caps relative to disks of equal geodesic radius—both captured in the covariant theory—qualitatively alters disclinations energetics.

The accuracy of both continuum elastic models can be tested by comparison to simulations of the bead-spring model introduced by Nelson and Seung (NS) [47]

$$E_{\text{NS}} = \frac{k}{2} \sum_{\langle i,j \rangle} (|\mathbf{r}_i - \mathbf{r}_j| - a)^2, \quad (4)$$

which consists of a triangular network of nearest neighbor springs of rest length  $a$  and spring constant  $k$ . As described in the Supplemental Material (specifically the software [34]), configurations possessing up to  $n_d = 0, 1, 2,$  or  $3$  fivefold disclinations are constructed by introducing multiple  $60^\circ$  Volterra cuts [27,48]. Figure 1 illustrates excellent agreement between the stress computed from the LF and simulation of a cap with a single off-center disclination, see the Supplemental Material for the details.

We first describe the elementary transition from the defect-free ground state to the ground state possessing the first stable internal disclination, with  $q = +1$ . For the FvK theory the elastic energy (per unit area) of the single-disclination cap is a function of the aperture angle  $\theta_c = W/R$ , the off-center defect position  $r$ , and the disclination charge  $q$  [28].

$$\frac{E_{\text{FvK}}}{YA} = \frac{\theta_c^4}{384} + \frac{1}{96} \left( \frac{q^2}{3} - \frac{q\theta_c^2}{2} \right) [1 - (r/W)^2]^2, \quad (5)$$

where the first term derives from curvature-generated stress, the second from the elastic self-energy of the disclination, and the third from the mutual elastic screening of the curvature and disclinations stress [49]. The expression for the elastic energy for the covariant energy,  $E_{\text{LF}}$ , is more complex as shown in the Supplemental Material [34] and described in Ref. [43] but reduces to Eq. (5) in the small-curvature limit,  $\theta_c \ll 1$ .

Because the self-energy and defect-curvature interactions exhibit exactly the same  $r$  dependence in the FvK theory, this model predicts a simple first order transition from the defect-expelled state (minimum at  $r^* \rightarrow W$ ) for  $\theta_c < \theta^*$  to the defect-centered state (minimum at  $r^* = 0$ ) for  $\theta_c > \theta^*$  at a critical cap angle  $\theta^* = \sqrt{2/3} \approx 0.816$ , see Fig. 2. Note that a standard heuristic argument [6] considers the cap angle,  $\theta_n$ , at which integrated Gaussian curvature “neutralizes” single fivefold defects [i.e., when  $\int dAs(\mathbf{x}) = \int dAK(\mathbf{x})$  yields cap angle  $\theta_n = \arccos(5/6) \approx 0.59$ ]. This “neutrality” angle falls well below the prediction for  $\theta^*$ , indicating that the cap requires significant “overcharging” by curvature-induced stress to overcome the self-energy of the monopole disclination.

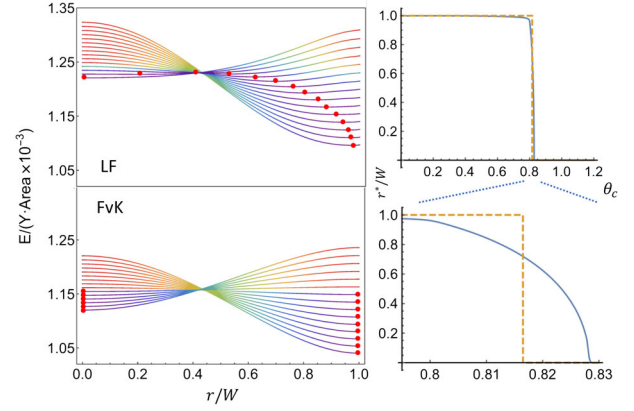


FIG. 2. Energy density vs the location of a disclination for different cap sizes. The red dots indicate the location of disclination that minimizes the energy density. Based on FvK, there is a first order transition from the edge to the center between  $\theta = 0.795$  and  $\theta = 0.83$ . However, there is a second order (smooth) transition from the edge to the center according to covariant theory.

Figure 2 illustrates the elastic energy vs defect position predicted by the (covariant) LF theory, where it is found that the first disclination emerges *continuously* from the boundary, starting approximately at  $\theta \approx 0.795$  reaching the center of the disk ( $r^* = 0$ ) at  $\theta \approx 0.83$ , exhibiting a range of off-center defect equilibria  $0 < r^* < W$  in this narrow curvature window [50].

The distinct first vs second order transitions predicted by the respective FvK and LF theories highlights the impact of the non-Euclidean embedding on the cap elasticity, even at fairly modest curvatures (i.e., well before the hemispherical geometry). While the FvK theory predicts the self-energy and defect-curvature interactions to precisely balance at the critical curvature, the appearance of stable off-center equilibrium for disclinations in the covariant theory can be associated with the imbalance between these two competing effects. Figure S2 plots the relative magnitudes of these terms, showing that (i) the defect self-energy is relatively depressed, while (ii) the defect-curvature is enhanced, as disclinations approach the free edge of the cap in the covariant theory relative to FvK. As discussed in more detail in Supplemental Material, Sec. I.C, the near-edge enhancement of curvature-generated attractions can be associated from the geometrically nonlinear edge compression, which grows faster than the small-slope (quadratic) approximation in FvK theory. On the other hand, the weakening of the repulsive self-energy is associated with the smaller geodesic curvature of the spherical cap (LF) edge compared to a planar disk (FvK), which amplifies the edge screening of defect stresses. These two geometric effects conspire to create “soft traps,” stabilizing off-center defect equilibria.

We note that the simulation model (Fig. S5b) shows a transition from defect-free to centered-disclination ground



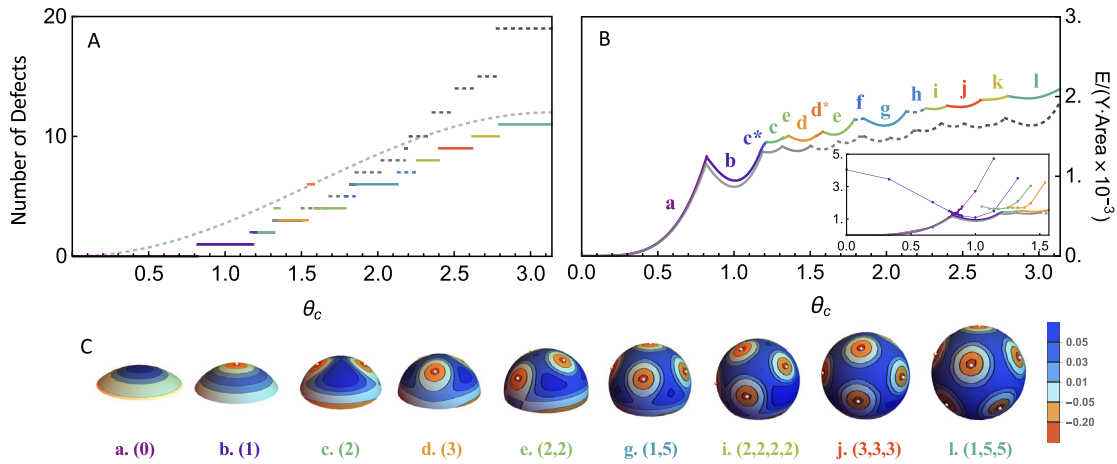


FIG. 3. Comparison of ground state energy and defects number in FvK vs LF. The colorful and dark gray lines correspond to the ground states obtained from LF and FvK theories. Only solid lines indicate the defect configurations follow IO symmetry. (a) Number of defects as a function of the growing cap size  $\theta_c$ . The dot-dashed line denotes to the topological charge neutrality condition. (b) Ground state energy as a function of cap size. The inset compares the ground state energy in simulation (dots) to LF (solid lines) and FvK (gray lines). (c) Stress distribution of the icosahedral subgroups emergent as the ground states in covariant theory.

state at a cap angle quite close to both continuum calculations,  $\theta^* \simeq 0.84$ . However, discreteness effects associated with the finite core size (zone of anharmonic strain) and noncircularity of the free edge obscure the resolution on the near-edge elastic binding of single defects.

We now consider the evolution of cap ground states from nearly flat ( $\theta_c \lesssim 1$ ) to closed shells ( $\theta_c \rightarrow \pi$ ). Previous considerations of the Thompson problem and its variants [17,19] point towards *icosahedral* defect configurations as ground states in closed spheres. Yet it remains unclear whether, and at what point, ground states of incomplete caps conform to this symmetry. Thus, we compare the elastic energy of two basic classes of disclination arrangements: first, patterns possessing subgroup symmetries of icosahedron (IO), as illustrated in a stereographic projection in Fig. S10; and, second, patterns composed of concentric  $n$ -fold symmetric rings of defects with composite symmetries listed in Table S1. For each configuration, energy is minimized with respect to the arc-radius of concentric rings of defects, retaining fixed azimuthal spacing between defects within each ring (see the Supplemental software [34]), and the rotation angle between concentric rings. For example, a (2,4) configuration is composed of two defects in the first ring and four defects in the second, in both cases evenly distributed. The elastic energy is then minimized with respect to the arc radius of two rings  $r_1, r_2$  and the rotation (phase) angle  $\phi$  between the rings.

We plot the results in terms of the number of *interior* disclinations and energy density of ground state configurations in Figs. 3(a) and 3(b), respectively, for both the FvK (black) and LF (color) elastic theories. Since their elastic energy contributions become arbitrarily small as defects approach the cap boundary, we introduce a cutoff radius of  $0.95W$ , beyond which we count defects to be at the boundary

of the crystal and not in the bulk. In the Supplemental Material, Fig. S9 shows that even large changes in this cutoff criterion lead to minor changes in the overall ground state landscape.

The defect number of LF ground states increases monotonically, with few exceptions (e.g., (2,2) and (3,3) following (2) and (3), respectively, due to the weak, near-edge defect traps) and always remains below the condition of topological charge neutrality (i.e., a number of internal defects whose total defect angle is equal to the integrated Gaussian curvature), with the calculation converging to the topologically correct condition of 12 defects with icosahedron symmetry for closed caps ( $\theta_c \rightarrow \pi$ ). In contrast, for  $\theta_c \gtrsim 2$  the ground states of the FvK model begin to greatly exceed the neutrality condition, eventually growing to +19 disclinations in the complete shell, far in excess of the +12 required on a closed sphere. In terms of the energy density [Fig. 3(b)], both theories show a similar crossover from the  $\sim \theta_c^4$  growth of elastic energy for defect-free caps to the plateaulike series of multidisclination minima at large coverage. Beyond the qualitative similarity in the curvature-dependence of the energy, the ground states symmetries of the two models differ substantially. As illustrated in Fig. 3(c), all but two ground states of the LF possess quasi-icosahedral symmetry. In contrast, as shown in the Supplemental Material, Fig. S8, ground states of the FvK theory with  $n_d > 3$  break icosahedral symmetry [with the sole exception of a narrow range of stable (3,3)] exhibiting higher-fold concentric-ring defect patterns that are also characteristic of planar vortex packings in superconducting ground states [32].

In summary, the detailed comparison of the widely used elastic plate theory (FvK), a covariant continuum elasticity theory (LF) and discrete lattice model (NS) of crystalline

caps reveal that qualitative features of the ground state structure and energetics derive from the non-Euclidean embedding of the elastic energy of caps, and, crucially, their free boundaries. Beyond modification of the transition from defect-free and defective caps at small curvatures, we find that the spherical embedding of this generalized jellium impacts the ground state symmetries, even at cap curvatures far from closure. Whereas the FvK model (i.e., “biharmonic, planar jellium”) predicts defect numbers and arrangements that depart wildly from structures predicted in closed shells [i.e.,  $n_d(\theta_c \rightarrow \pi) \gg 12$ ], the ground states covariant LF model (i.e., “biharmonic, spherical jellium”) rather smoothly interpolate to the icosahedral arrangements of 12  $q = +1$  defects for  $\theta_c \rightarrow \pi$ . This shows that topological constraint that applies for *closed shells* (i.e.,  $\sum_{i=1}^{n_d} q_i = 12$ ) is not strictly necessary for the stability of icosahedral defect arrangements; such ground states can emerge purely from the (topologically unconstrained) energetics of multidefect arrangements on *incomplete shells*, but only when embedded properly in a spherical geometry.

A recent study showed that nearly IO arrangements emerge from nonequilibrium models of crystalline shell growth in which defects can only form at the free edge of growing cap [24]. The present results show that these kinetically accessible structures are, indeed, remarkably close to the ground states of axisymmetric, and partially closed caps, over the full range of curvature (see discussion in the Supplemental Material [34]). More broadly, the evolution of the ground state structure from flat to closed shells forms the basis for addressing more complex models of shell structure. For example, models describing the decoration of isolated positive disclinations with an excess of five to seven dislocation pairs in large- $N$  crystals as well as an anisotropic boundary shape in the limit of low edge energy to modulus ratios [21,22,25,36,37] have, until now, only addressed the “small-slope” limits accessible via FvK theory. The present results argue that capturing the full geometric nonlinearity of defect elasticity will be equally essential for understanding more complex partial-shell morphologies, even at qualitative level, far from the weakly curved regime.

The authors are grateful to the hospitality of Aspen Center for Physics (NSF PHY 1607611) where this work began. The work of S. L. and R. Z. was supported by the NSF through Grant No. DMR-1719550. A. T. acknowledges support from NSF through Grant No. DMR-1606336 and G. G. from the DOE Office of Science, Basic Energy Sciences, under Award No. DE-SC0017870.

- 
- [1] D. L. Caspar and A. Klug, *Cold Spring Harbor Symp. Quant. Biol.* **27**, 1 (1962).  
 [2] H. W. Kroto, J. R. Heath, S. C. O’Brien, R. F. Curl, and R. E. Smalley, *Nature (London)* **318**, 162 (1985).

- [3] R. Zandi, D. Reguera, R. F. Bruinsma, W. M. Gelbart, and J. Rudnick, *Proc. Natl. Acad. Sci. U.S.A.* **101**, 15556 (2004).  
 [4] S. Panahandeh, S. Li, and R. Zandi, *Nanoscale* **10**, 22802 (2018).  
 [5] A. Bausch, M. Bowick, A. Cacciuto, A. Dinsmore, M. Hsu, D. Nelson, M. Nikolaidis, A. Travasset, and D. Weitz, *Science* **299**, 1716 (2003).  
 [6] W. T. Irvine, V. Vitelli, and P. M. Chaikin, *Nature (London)* **468**, 947 (2010).  
 [7] S. Guttman, Z. Sapir, M. Schultz, A. V. Butenko, B. M. Ocko, M. Deutsch, and E. Sloutskin, *Proc. Natl. Acad. Sci. U.S.A.* **113**, 493 (2016).  
 [8] A. Bandekar and S. Sofou, *Langmuir* **28**, 4113 (2012).  
 [9] D. Chen and M. M. Santore, *Proc. Natl. Acad. Sci. U.S.A.* **111**, 179 (2014).  
 [10] S. Smale, *Math. Intell.* **20**, 7 (1998).  
 [11] A. Pérez-Garrido, M. J. W. Dodgson, and M. A. Moore, *Phys. Rev. B* **56**, 3640 (1997).  
 [12] D. R. Nelson, *Defects and Geometry in Condensed Matter Physics* (Cambridge University Press, Cambridge, England, 2002).  
 [13] M. Kléman, *Adv. Phys.* **38**, 605 (1989).  
 [14] M. J. Bowick, D. R. Nelson, and A. Travasset, *Phys. Rev. B* **62**, 8738 (2000).  
 [15] V. Vitelli, J. B. Lucks, and D. R. Nelson, *Proc. Natl. Acad. Sci. U.S.A.* **103**, 12323 (2006).  
 [16] J. Wagner and R. Zandi, *Biophys. J.* **109**, 956 (2015).  
 [17] M. J. Bowick and L. Giomi, *Adv. Phys.* **58**, 449 (2009).  
 [18] E. L. Altschuler, T. J. Williams, E. R. Ratner, F. Dowla, and F. Wooten, *Phys. Rev. Lett.* **72**, 2671 (1994).  
 [19] M. Bowick, A. Cacciuto, D. R. Nelson, and A. Travasset, *Phys. Rev. Lett.* **89**, 185502 (2002).  
 [20] D. J. Wales, H. McKay, and E. L. Altschuler, *Phys. Rev. B* **79**, 224115 (2009).  
 [21] A. Azadi and G. M. Grason, *Phys. Rev. Lett.* **112**, 225502 (2014).  
 [22] A. Azadi and G. M. Grason, *Phys. Rev. E* **94**, 013003 (2016).  
 [23] M. Castelnovo, *Phys. Rev. E* **95**, 052405 (2017).  
 [24] S. Li, P. Roy, A. Travasset, and R. Zandi, *Proc. Natl. Acad. Sci. U.S.A.* **115**, 10971 (2018).  
 [25] S. Schneider and G. Gompper, *Europhys. Lett.* **70**, 136 (2005).  
 [26] L. Giomi and M. Bowick, *Phys. Rev. B* **76**, 054106 (2007).  
 [27] G. M. Grason, *Phys. Rev. Lett.* **105**, 045502 (2010).  
 [28] G. M. Grason, *Phys. Rev. E* **85**, 031603 (2012).  
 [29] L. Bonsall and A. A. Maradudin, *Phys. Rev. B* **15**, 1959 (1977).  
 [30] D. S. Fisher, B. I. Halperin, and R. Morf, *Phys. Rev. B* **20**, 4692 (1979).  
 [31] A. K. Geim, I. V. Grigorieva, S. V. Dubonos, J. G. S. Lok, J. C. Maan, A. E. Filippov, and P. F. Maan, *Nature (London)* **390**, 259 (1997).  
 [32] B. J. Baelus, F. M. Peeters, and V. A. Schweigert, *Phys. Rev. B* **63**, 144517 (2001).  
 [33] V. A. Schweigert, F. M. Peeters, and P. S. Deo, *Phys. Rev. Lett.* **81**, 2783 (1998).  
 [34] See the Supplemental Material at <http://link.aps.org/supplemental/10.1103/PhysRevLett.123.145501> for details on Mathematica notebooks for simulation of caps with 0-3 disclinations and for computation of defect ground states from continuum models.

- [35] A. Y. Morozov and R. F. Bruinsma, *Phys. Rev. E* **81**, 041925 (2010).
- [36] G. Meng, J. Paulose, D. R. Nelson, and V. N. Manoharan, *Science* **343**, 634 (2014).
- [37] D. M. Hall and G. M. Grason, *Interface Focus* **7**, 20160140 (2017).
- [38] We expect this boundary shape instability is suppressed in the limit of edge energies much larger than  $\sim Y\theta_c^4 W$  [35,37,39].
- [39] R. Zandi, P. van der Schoot, D. Reguera, W. Kegel, and H. Reiss, *Biophys. J.* **90**, 1939 (2006).
- [40] The derivations for FvK in axisymmetric 2D crystals were originally applied to twisted columnar phases, the elastic energy of which is identical to crystalline caps in the small-slope, or low-twist, regimes.
- [41] L. Landau and E. Lifshitz, *Theory of Elasticity* (Butterworth-Heinemann, Oxford, 1986), Vol. 7.
- [42] G. M. Grason, *J. Chem. Phys.* **145**, 110901 (2016).
- [43] S. Li, R. Zandi, and A. Travasset, *Phys. Rev. E* **99**, 063005 (2019).
- [44] E. Efrati, E. Sharon, and R. Kupferman, *J. Mech. Phys. Solids* **57**, 762 (2009).
- [45] M. Moshe, E. Sharon, and R. Kupferman, *Phys. Rev. E* **92**, 062403 (2015).
- [46] A. E. Romanov, *Phys. Status Solidi (a)* **63**, 109 (1981).
- [47] H. S. Seung and D. R. Nelson, *Phys. Rev. A* **38**, 1005 (1988).
- [48] A. Travasset, *Phys. Rev. B* **68**, 115421 (2003).
- [49] Note that we neglect in this analysis the core energy of disclinations, which is expected on dimensional grounds to be comparable to  $\sim Ya^2$  and hence much smaller than the far-field, elastic energies of disclinations,  $\sim YW^2$ .
- [50] We point out that, in Ref. [24], the appearance of the first defect was reported to be at  $\theta \simeq 0.66$  instead of 0.795 due to numerical error introduced by summing over not enough modes in the multipole expansion of self-energy. See Fig. S1.